

Determination of the whole set of elastic constants of a polymeric Langmuir-Blodgett film by Brillouin spectroscopy

Fabrizio Nizzoli,* Burkard Hillebrands,[†] Sukmock Lee, George I. Stegeman, Gisela Duda,[‡] Gerhard Wegner,[‡] and Wolfgang Knoll[‡]

Optical Sciences Center, University of Arizona, Tucson, Arizona 85721

(Received 13 January 1989)

We report Brillouin light scattering experiments on polymeric uniaxial Langmuir-Blodgett films, which have their preferred axis, the c axis, in the plane of the film. Both acoustic surface and bulk modes were observed. In addition to the usual Rayleigh and Sezawa film modes, a longitudinal guided acoustic phonon was identified. Also observed, and verified by computer simulations, was a resonant enhancement of the scattering cross section for some Sezawa modes due to an additional bulk coupling mechanism of the scattered light to the film modes. The complete set of elastic constants as well as the refractive indices were determined from the spectra. For the samples that we had measured, with more than ten molecular monolayers, the elastic constants do not depend on the film thickness. The ratio between the transverse and the longitudinal sound velocities is found to be much smaller than for ordinary solids.

INTRODUCTION

The elastic properties of Langmuir-Blodgett (LB) films are very difficult to measure, both due to their fragile nature and due to the film fabrication technique which requires that they are grown onto a solid support. Brillouin light scattering, that is, inelastic scattering of light from propagating surface or bulk phonons, is the only nondestructive experimental technique for measuring several elastic constants of these materials. So far there are only a few reports on the measurement of elastic constants of LB films. For Cd-arachidate (CdA) LB films three elastic constants were measured and upper limits were found for the other three elastic constants.¹ For unpolymerized and polymerized ODF and ODM LB films the elastic constants have been determined.²

In the present work, multilayer assemblies of performed polymers³ are investigated. These new LB materials have attracted considerable interest due to their improved thermal and mechanical stability. Moreover, new structural concepts and their implications for the fabrication of multilayers are studied with these systems. The polyglutamates with long alkyl side chains [poly(γ -methyl-L-glutamate-co- γ - n -alkyl-L-glutamate)] employed in our studies have been shown to form stable monolayers on the water surface if the polyglutamate backbone can adopt a helical configuration and the hydrocarbon chains are in a liquid-crystalline-analogous state. These rodlike molecules orient parallel to the dipping direction during the transfer to the solid substrate. This geometry allows films which are strongly anisotropic in the surface plane to be studied. Therefore much more information can be obtained relative to the previous cases^{1,2} where the molecules were aligned perpendicular to the surface, resulting in films with uniaxial, elastically hexagonal, structures with c axis normal to the surface.

EXPERIMENT

The Brillouin light scattering experiments were performed in air at room temperature. Light from a single-mode 514.5-nm Ar⁺ laser, polarized in the scattering plane, was focused onto the LB films at a variety of angles of incidence, and 180° backscattered light was collected and analyzed using a Sandercock-type, high-contrast, (3+3)-pass tandem Fabry-Perot interferometer. The laser power at the sample surface was typically less than 25 mW to avoid surface damage of the samples.

The synthesis of poly(γ -methyl-L-glutamate-co- γ - n -octadecyl-L-glutamate) has been described elsewhere.³ The average degree of polymerization is $P_n = 136$. The content of randomly occurring octadecyl-L-glutamate residues is 32 mol.% and the average length of the helical rods is 20 nm. The transfer of the monolayer from the water surface to the solid substrate as Y-type LB multilayers was performed at a lateral pressure $\Pi = 25$ mN m⁻¹ where the film is in a liquid-crystalline state at an area per repeat unit of $A = 0.20$ nm². The molybdenum substrates were first coated with one monolayer of arachidate [CH₃—(CH₂)—COO—] in order to render them hydrophobic. Up to 560 monolayers could be deposited at a rate of 20 nm/min. The average monolayer thickness obtained by small-angle x-ray scattering (SAXS) measurements³ was $d = 1.75$ nm. The anisotropic index of refraction was determined in a separate experiment by an optical waveguide technique.⁴ We obtained $n_{\parallel} = 1.54 \pm 0.02$, $n_{\perp} = 1.47 \pm 0.02$, and $n_{o.p.} = 1.39 \pm 0.03$ (for definitions of the indices see Fig. 1). As shown before,³ these results indicate an orientation of the rodlike molecules with their long axis parallel to the dipping direction. A schematic picture of the resulting structure for a double layer of polyglutamate is given in Fig. 1. The density of the LB film was estimated from the sur-

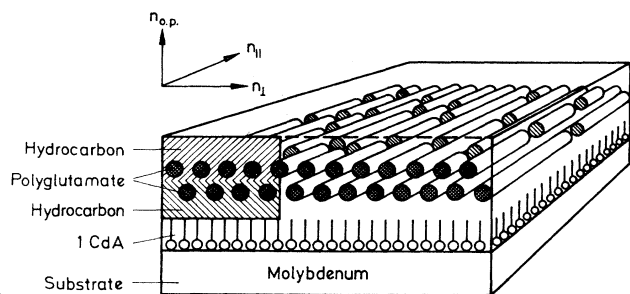


FIG. 1. Schematic diagram of the organization of a double layer of polyglutamate on a solid support. The substrate is polished molybdenum which is coated with one monolayer of arachidate. Onto this hydrophobic surface a Y-type LB layer is deposited. The long axis of the rodlike helical glutamate backbone is aligned parallel to the dipping direction during transfer. Given in the inset is also the definition of the three indices of refraction.

face area per repeat unit on the water surface at the transfer pressure, and the thickness of the deposited monolayer. We obtained $\rho = 1.156 \text{ g cm}^{-3}$.

RESULTS AND DISCUSSION

The LB films used in the experiments were deposited on a molybdenum substrate. For a transparent film on an opaque substrate the Brillouin cross section contains, in principle, contributions from both bulk and surface acoustic excitations. The light couples to the thermally excited phonon modes through the phonon-induced modulation of the dielectric tensor of the film (elasto-optic-mechanism) and through the dynamical corrugations of the film interfaces (ripple effect).⁵ One therefore expects that Brillouin spectra from such films carry a rich amount of information. In addition the propagation velocities of the bulk modes in the soft LB films are much lower than the corresponding quantities of the Mo substrate.¹ This provides for a large number of guided acoustic modes in the supported film (Sezawa or generalized Lamb waves).

In the following we use a coordinate system which is aligned with the molecular axis. The c axis (a axis) is in plane, and parallel (perpendicular) to the molecule axis; the b axis is perpendicular to the film. Therefore, c_{33} (c_{11}) is the longitudinal elastic modulus for phonon propagation parallel to the film, and parallel (perpendicular) to the molecular axis, and c_{22} is the longitudinal elastic modulus for propagation along the film normal.

The analysis of the Brillouin spectra requires a clear identification of the bulk and surface modes which overlap frequently in LB films due to the small index of refraction of these films. In the spectra, a bulk mode in a transparent medium gives rise to a sharp line of frequency

$$\Omega_B = \frac{4\pi}{\lambda} n v_B, \quad (1)$$

where λ is the wavelength of the light, n is the index of refraction, and v_B is the propagation velocity of the bulk mode. Conversely a surface mode is characterized by a frequency shift

$$\Omega = Q_{\parallel} v_S, \quad (2)$$

where v_S is the velocity of the surface mode and $Q_{\parallel} = (4\pi/\lambda)\sin\theta$ is the surface wave vector, defined by the scattering geometry. θ is the angle between the incoming light beam and the surface normal. An additional way of interaction of light with film phonons should be discussed. The laser beam reflected from the Mo interface can give rise to scattering of phonons with wave vectors parallel to the film, which also satisfies Eq. (2). This scattering channel, as well as its inverse, is also included in the theory.

The determination of the elastic constants of the LB films is largely based on the data in Fig. 2, which have been taken in a thick supported LB film for different angles of incidence. For data set (a), Q_{\parallel} is perpendicular to the axis of the organic molecules, while for set (b), Q_{\parallel} is parallel to this axis. As expected, the two sets of spectra are very different due to the strong anisotropy of the film.

The set of spectra (a) shows two peaks, except for $\theta = 0^\circ$. The peak at about 12 GHz is assigned as a longitudinal bulk mode of almost constant velocity v_L . The frequency of the other peak shifts as $\sin\theta$, so that it is identified as a surface mode of velocity v_S .

It has been recently found⁶ in transparent supported films, for example, 1 and 2 μm ZnSe on GaAs, that the Brillouin spectra show a sharp line just above the frequency shift associated with the longitudinal wave velocity, due to scattering from a longitudinal guided mode (LGM). The observed surface mode is in the right frequency range and it is therefore assigned as a first-order LGM. A displacement-field calculation in the film will be presented later which confirms this hypothesis. The present case differs from that of the ZnSe film: there the

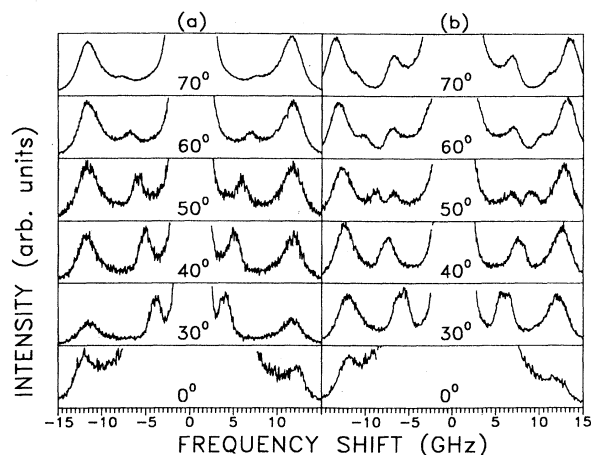


FIG. 2. Brillouin spectra obtained from LB films on molybdenum. Film thickness $h = 9825 \text{ \AA}$. (a) Q_{\parallel} perpendicular to the molecular axis. (b) Q_{\parallel} parallel to the molecular axis.

LGM was a leaky mode, here in the present case the LGM is well below the transverse velocity of molybdenum and therefore it belongs to the discrete spectrum.

Note that by changing θ in data set (a), the detected longitudinal bulk mode travels along different directions perpendicular to the axis of the molecules. The lack of dispersion with direction allows us to draw an important conclusion concerning the crystal symmetry of the LB film. Because the longitudinal bulk mode has constant velocity v_L , the LB film can be modeled as a hexagonal crystal with the c axis parallel to the surface. This is also in agreement with the lack of observation in data set (a) of Fig. 2 of a transverse bulk mode; in fact, in the basal plane of a hexagonal crystal the three acoustic modes are pure modes and the symmetry forbids the detection of a pure transverse mode in p - p backscattering. All of these arguments lead to the conclusion that $v_S = v_L$ and that simply $v_L = (c_{11}/\rho)^{1/2}$. Now it is possible from the frequency of the LGM in the data set of Fig. 2(a) and from Eq. (2) to calculate the longitudinal velocity for propagation in the basal plane of the LB crystal, i.e., $v_L = 2025$ m/sec. Because the density ρ of the LB film is known to be equal to 1.156 g/cm³, we directly calculate $c_{11} = 4.74$ GPa.

Data set (a) of Fig. 2 also contains important information on the index of refraction, n , of the LB film. In our scattering geometry the electric field of the light is always perpendicular to the c axis of the hexagonal LB film, so that in this case n is to be replaced by the basal-plane component $n_{\perp} \equiv n_{o.p.}$ in Eq. (1). Using the measured value of v_L from the LGM, Eq. (1) gives $n_{\perp} = 1.48$, which is in good agreement with the result obtained from the optical waveguide experiment.⁴

The mode velocities in a plane perpendicular to the molecular axis depend, within the hexagonal model, on two additional independent elastic constants, i.e., c_{11} and c_{66} . For this case $c_{11} - c_{12} = c_{66}$. More data are necessary to determine c_{66} . In Fig. 3 we show a large number of data points taken at different angles θ and for different film thicknesses $h = 200, 410, 795, 1600, 3525,$ and 9825 Å. A best fit to the data points of the two lowest-order modes (Rayleigh and Sezawa waves) gives $c_{66} = 0.66$ GPa and consequently $c_{12} = 3.43$ GPa. The calculated dispersion curves in Fig. 3 have been generated with the above values of $c_{11}, c_{12},$ and c_{66} . The overall agreement is good.

The LGM deserves additional comments. The data points in Fig. 3 in the velocity range 2000–2100 m/sec and for $5 \leq Q_{\parallel}h \leq 23$ are assigned as the LGM. These data refer to films of thicknesses of 3525 and 9825 Å. It is interesting to note that the LGM is well defined when $Q_{\parallel}h \geq 2\pi$, i.e., for a film thickness h greater than the surface-phonon wavelength. By inspecting the dispersion curves of Fig. 3 it is evident that the experimental points due to the LGM lie at the intersection of a horizontal line [representing to a good approximation the existence condition of the LGM (Ref. 6)] with the dispersion relations of the Sezawa modes of the supported film. The calculated curves show a "bunching" of modes close to v_L , due to a form of hybridization between the LGM and the Sezawa modes. Because the dispersion curves cannot in-

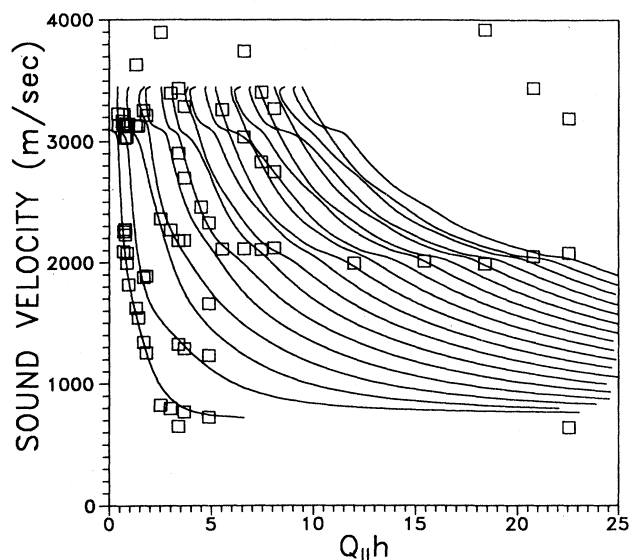


FIG. 3. Measured dispersion relations of several guided modes in LB films for different thicknesses and scattering angles (squares). Measurements performed with Q_{\parallel} perpendicular to the molecular axis. The solid lines are the calculated dispersion curves with the elastic constants of Table I.

intersect, they produce an alternate sequence of gaps and plateaus. A similar behavior also occurs at about 3100 m/sec. In this case, as already noted,¹ the flat dispersion curve which is responsible for this effect is the Rayleigh wave (RW) of the substrate.

For very large film thicknesses the LGM becomes a longitudinal bulk mode traveling parallel to the film. For the film-thickness regime considered in this work no real bulk modes do exist in the film.

In order to corroborate the assignment of the modes, we show in Figs. 4 and 5 the displacement-field amplitudes for the two modes of interest. Figure 4 refers to a mode with $Q_{\parallel}h = 22.55$ and $v = 2047$ m/sec. The calculation shows a pattern typical of the LGM,⁶ with a strong localization of the longitudinal displacements in the central part of the film and very small transverse displacements. Figure 5 refers to a mode with $Q_{\parallel}h = 6.6$ and $v = 3034$ m/sec, close to the RW velocity of the free substrate. This mode is characterized by the usual oscillatory behavior of the displacement field for guided modes. The polarization of the mode at the two film interfaces is mainly shear vertical. We found that the localization at the film-Mo interface is particularly strong compared to that of the neighboring modes for the same value of $Q_{\parallel}h$. Therefore the ripple contribution to the scattering intensity is very large at the interface for this mode. The strong localization at the interfaces is reminiscent of the fulfillment of the stress-free boundary condition of the free Mo surface for the RW velocity, which is close to that of the Sezawa mode in the film.

Finally the three experimental points in the top right-hand corner of Fig. 3 represent scattering from the longitudinal bulk mode of constant frequency. Although at

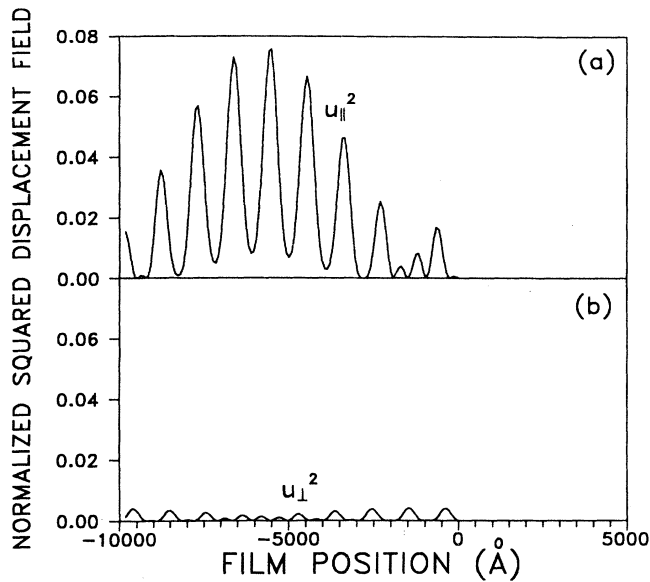


FIG. 4. Calculated squared displacement field for a mode of velocity $v = 2047$ m/sec in a 9825-Å LB film on molybdenum. $Q_{\parallel} = 0.0023 \text{ \AA}^{-1}$. The negative values of the abscissa refer to the film, whereas the positive values refer to the substrate. The ordinate is the squares of the amplitude component (a) parallel and (b) perpendicular to the surface.

first sight the representation of bulk modes in a surface-wave graph as in Fig. 3 seems meaningless, we will show later that it is useful indeed, because it reveals the actual mechanism of interaction of the light with "bulk" modes in supported films of finite thickness.

We now analyze data set (b) of Fig. 2. Here the situation is more complicated than for set (a) for many

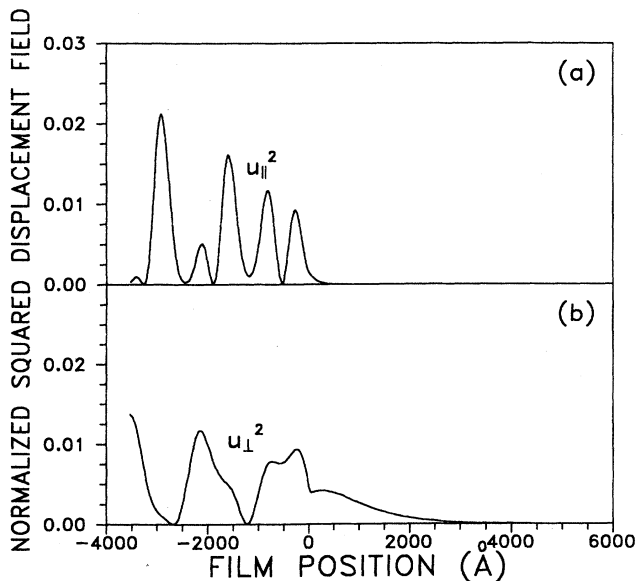


FIG. 5. As in Fig. 3 but for a 3525-Å LB film on molybdenum. $Q_{\parallel} = 0.00187 \text{ \AA}^{-1}$. Mode velocity $v = 3034$ m/sec.

reasons. We expect two bulk peaks to be present in the spectra because, by changing θ , the light scans different phonon wave vectors in a plane containing the c axis of the hexagonal LB film (meridian plane). In such a plane there are two modes detectable in a p - p scattering: one polarized mainly longitudinal and one mainly shear vertical. A further complication arises because the propagation direction of the light inside the material depends on both components of the refractive index n_{\perp} and n_{\parallel} . In addition, the spectra should show a LGM, whose velocity is given in this case by $(c_{33}/\rho)^{1/2}$.

The peak in Fig. 2(b) marked as LGM was identified as a longitudinal guided mode because it obeys Eq. (2). We therefore find $c_{33} = 10.8$ GPa. The quasilongitudinal bulk mode is responsible for the peak whose frequency changes from 12 to 13 GHz when θ varies from 0° to 70° . The quasitransverse bulk mode gives rise to a well-defined peak at about 6.5 GHz for $\theta = 50^{\circ}$, 60° , and 70° . For $\theta < 50^{\circ}$ it is obscured by the LGM.

The modes in Fig. 2(b) depend on c_{11} , c_{33} , c_{13} , and c_{44} . Because c_{11} and c_{33} have been already determined, only c_{13} and c_{44} need to be obtained by fitting to the data. Actually the data of Fig. 2(b) allow a precise determination of c_{13} and c_{44} , once n_{\parallel} is known. We have found that the calculated values of c_{44} strongly depend on n_{\parallel} . A variation on n_{\parallel} of 1% changes the calculated c_{44} by about 12%. Now it is c_{44} which mainly determines the RW velocity in the film. The RW does not appear in Fig. 2, but has been measured using a smaller free spectral range for Q_{\parallel} parallel to the molecular axis. The experimental data for different angles θ and different film thicknesses are reported in Fig. 6. In order to reproduce both the bulk

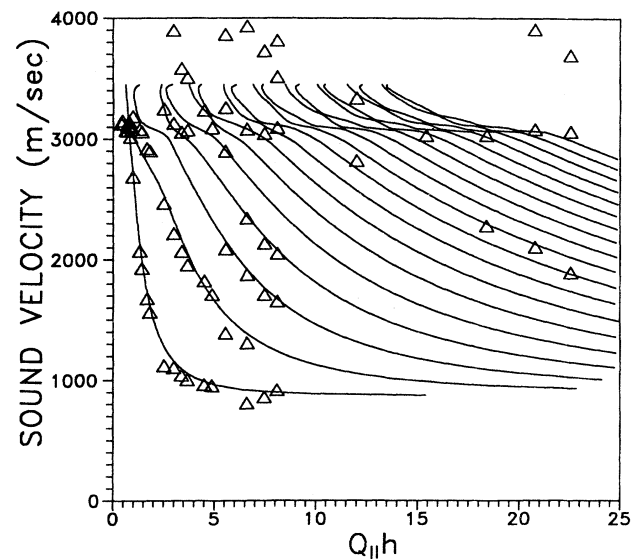


FIG. 6. Measured dispersion relations of several guided modes in LB films for different thicknesses and scattering angles (triangles). Measurements performed with Q_{\parallel} parallel to the molecular axis. The solid lines are the calculated dispersion curves with the elastic constants of Table I.

peaks in Fig. 2(b) and the RW in Fig. 6 we had to choose the following values: $c_{44}=0.91$ GPa, $c_{13}=3.57$ GPa, $n_{\parallel}=1.48$. The latter value of n_{\parallel} deviates from the result obtained with the optical waveguide technique by less than 4%, which is within the error margins. The whole set of elastic constants of the LB films has therefore been determined. The results are summarized in Table I. The error in the evaluation of the elastic constants can be estimated to be around 5%. The elastic constants of Table I have been used to generate the calculated dispersion relations of Rayleigh and Sezawa modes in Fig. 6. The overall agreement with the experimental data is remarkable. The "bunching" of the dispersion relations close to 3100 m/sec is due to the combined effect of the RW of molybdenum and of the LGM of the LB film. They turn out to have, in this case, almost the same velocity. However the calculated displacement field for $Q_{\parallel}h \geq 2\pi$ is typical of the LGM, while only for small film thicknesses it is reminiscent of the RW of the substrate.

Let us now consider in detail the interaction of the light with what we have called "bulk" modes in the LB film of thickness $h=9825$ Å. For this finite thickness, the propagation in the film of the full continuum of bulk modes of the infinite medium is not allowed rigorously. For a given Q_{\parallel} the perpendicular components of the acoustic wave vector is "quantized" and only the modes that satisfy the surface boundary conditions are allowed.⁷ Therefore, given the refractive index and the angle θ , the light beam inside the transparent film is not necessarily aligned with an allowed "bulk" transverse or longitudinal phonon that satisfies the total wave-vector conservation condition for backscattering in bulk media. However, there will be one Sezawa mode whose transverse or longitudinal wave-vector component is almost aligned with the wave vector of the light required for Bragg backscattering. Therefore we believe that the "bulk" modes measured in the experiments actually coincide approximately with one Sezawa mode, due to the complete wave-vector conservation throughout the film, whose Brillouin elasto-optic cross section is strongly enhanced. This is illustrated in Fig. 6. The three experimental points centered around $Q_{\parallel}h \approx 20$ and $v \approx 2000$ m/sec correspond to the constant frequency peaks at about 6.5 GHz in Fig. 2(b) for $\theta=50^\circ$, 60° , and 70° . These experimental points lie on particular high-order Sezawa modes, whose elasto-optic cross sections are large because the total wave vector is approximately conserved in the scattering process. This effect is accounted for by the theory of Brillouin scattering in a supported film.⁵ For thick films the spectrum of the guided modes is quasicontinuous: this explains why the Sezawa modes accurately represent the bulk modes of the semi-infinite medium in the case of

TABLE I. Measured elastic constants of the LB films (in GPa). The coordinate system is aligned along the molecule axes, i.e., the c axis is along the molecule axis in the film plane.

c_{11}	c_{33}	c_{12}	c_{13}	c_{44}	c_{66}
4.74	10.8	3.43	3.57	0.91	0.66

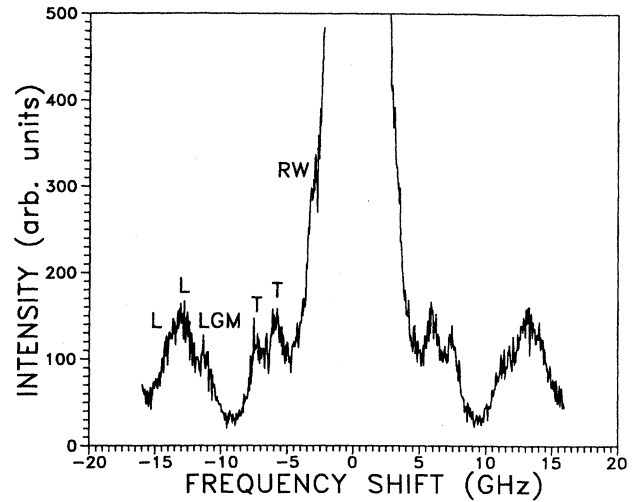


FIG. 7. Experimental Brillouin spectrum for a LB film of thickness $h=3525$ Å and scattering angle $\theta=70^\circ$.

the 9825-Å LB film. In a thinner film, e.g., the 3525-Å LB film with $Q_{\parallel}h \approx 8.1$ in Fig. 6, the discreteness of the guided-mode spectrum becomes relevant and the more or less resolved double-peaked structure occurs due to scattering from two Sezawa modes. Figure 7 exemplifies such a case. Here the two peaks marked T are due to two Sezawa modes close to the "bulk" Bragg condition for quasitransverse phonons. In other words, the sharp bulk peak expected in the semi-infinite medium has "split" due to the finite thickness of the film. The broad high-frequency structure contains contributions from the LGM and from two leaky Lamb modes (L) whose frequencies are close to the Bragg condition for a quasilongitudinal bulk mode.

Within the cubic crystal approximation of the theory outlined in Ref. 5, we were able to fit also the intensities of a few Brillouin spectra with a reasonable choice of the elasto-optic constants k_{ij} of the LB film ($|k_{ij}| \leq 3$). However, we found it impossible to reproduce with a single set of elasto-optic constants all the available spectra. This would require a consistent theory of the elasto-optic interaction in hexagonal films, which has not been developed to date.

CONCLUSIONS

Polymeric LB films deposited on a molybdenum substrate with the molecular axes parallel to the surface were found to form a crystal of hexagonal symmetry with the c axis parallel to the surface. Brillouin spectra taken at different scattering angles and for film thickness in the range 200–9825 Å show peaks corresponding to the surface Rayleigh wave and to several guided modes (Sezawa and longitudinal guided). In the thickest film (9825 Å), well-defined bulk modes were also observed. The peaks in the spectra have been unambiguously assigned and the whole set of elastic constants of the LB films has been calculated from the position of the spectral lines. This set of

elastic constants explains the data for all samples of different thicknesses. We conclude that the elastic constants of these films do not depend on the number of layers in the films, at least for more than 10 layers. The ratio between the transverse elastic constants c_{44} and c_{66} and the longitudinal elastic constants c_{11} and c_{33} is much smaller than in ordinary solids. It is indicative for a partially fluidlike behavior of the LB film, as also suggested by the film structure.

By comparing the Brillouin shifts of surface and bulk modes we also determined the two components $n_{\perp} \equiv n_{o.p.}$ and n_{\parallel} of the index of refraction, which appears to be isotropic, within the accuracy of the measurements. Conversely, calculations of the scattering cross section have

shown that the elasto-optic tensor of the LB film must be quite anisotropic in order to explain the whole set of available data.

ACKNOWLEDGMENTS

This work was supported by the U.S. Air Force Office of Scientific Research—University Research Initiative Program under Contract No. F49620-86-C-0123. F. N. acknowledges research support from Ministero della Pubblica Istruzione (MPI 40% Unità di Ricerca del Centro Interuniversitario di Struttura della Materia—Università degli Studi di Modena) and Consiglio Nazionale della Ricerche (travel grant).

*Permanent address: Dipartimento di Matematica e Fisica, Università degli Studi di Camerino, I-62032 Camerino, Italy.

†Present address: II. Physikalisches Institut, Rheinisch-Westfälische Technische Hochschule Aachen, Templergraben 55, D-5100 Aachen 1, Federal Republic of Germany.

‡Permanent address: Max-Planck-Institut für Polymerforschung, Jakob-Welder-Weg 11, D-6500 Mainz, Federal Republic of Germany.

¹R. Zanoni, C. Naselli, J. Bell, G. I. Stegeman, and C. T. Seaton, *Phys. Rev. Lett.* **57**, 2838 (1986).

²S. Lee, B. Hillebrands, G. I. Stegeman, L. A. Laxhuber, and G.

D. Swalen, *J. Chem. Phys.* (to be published).

³G. Duda, A. J. Schouten, T. Arndt, G. Lieser, G. F. Schmidt, C. Bubeck, and G. Wegner, *Thin Solid Films* **159** (1988).

⁴W. Hickel, G. Duda, G. Wegner, M. Jurich, J. S. Swalen, K. Rochford, G. I. Stegeman, and W. Knoll (unpublished).

⁵V. Bortolani, A. Marvin, F. Nizzoli, and G. Santoro, *J. Phys. C* **16**, 1757 (1983).

⁶B. Hillebrands, S. Lee, G. I. Stegeman, H. Cheng, J. E. Potts, and F. Nizzoli, *Phys. Rev. Lett.* **60**, 832 (1988).

⁷B. A. Auld, *Acoustic Fields and Waves in Solids* (Wiley, New York, 1973), Vol. 2.